JOURNAL OF MATERIALS SCIENCE 2 (1967) 40 - 45

On the Structure and Lattice Faults of Electrodeposited Nickel

E. J. SUONINEN
Institute of Technical Physics, University of Oulu, Oulu, Finland

Received 24 October 1966

The influence of bath pH on the structure and lattice faults of nickel deposited from a sulphate bath was investigated by X-ray diffraction. A special method was developed for separating the effects of macrostrains and deformation stacking faults on the peak positions.

Measurable amounts of twin faults and macrostrains along the cube edges were found in samples kept at room temperature. No deformation faults or strains along the cube diagonals were found. The faults and the strains disappeared by heating to about 300 to 400° C. The coherent domain size was also found to increase in the same region.

Most of the phenomena observed were probably caused by co-deposition of colloidal nickel hydroxide into the cathode. The twin faults were possibly caused, at least indirectly, by co-deposited hydrogen.

1. Electrolysis of Nickel*

It is well known that electrolytic deposits of nickel usually exhibit large tensile stresses which often cause severe technical difficulties. Another phenomenon characteristic of the electrolysis of nickel is the low overvoltage of hydrogen. The overvoltage of nickel itself is, on the other hand, relatively high, indicating some kind of inhibition mechanism to be present in the electrodeposition of nickel even in the absence of impurities.

The above observations can be considered in the light of various existing theories on the factors controlling the deposition and the resulting structure. In particular, two specific factors must be taken into account: the effects of hydrogen ions and of colloidal nickel hydroxide. Hydrogen ions are capable of co-depositing as neutral atoms into the cathode because of their small overvoltage and must be regarded as a possible source of various kinds of lattice imperfections which in turn create the stresses observed. On the other hand, colloidal nickel hydroxide is known to exist in electrolytes of moderate or weak acidity in which the electrolysis is usually performed. The colloid probably acts as an inhibitor for the deposition of nickel, the high overvoltage of which is thus explained. Since the colloidal particles are known to carry a positive charge, they can be drawn into the cathode and co-deposited into the nickel lattice. This would naturally also explain the stresses observed.

Both of the above-described mechanisms can be expected to depend on the pH value of the bath. Hence, both can explain the fact that various characteristics of the electrolysis of nickel, especially the resulting structure, are indeed found to depend in a very sensitive way on pH. On the other hand, it is not easy to decide which of the two mechanisms is responsible for the characteristic properties of the deposit. A conclusive decision of the matter can be greatly facilitated by a more detailed knowledge of the structure and lattice faults of the deposit, since these can be expected to reflect the mechanism creating them.

2. X-ray Methods

During the last decade, studies of the structure of electrodeposited metal layers have gained new impetus through the use of the well-known, X-ray diffraction methods based on quantitative

*A thorough treatment of the electrolysis of nickel can be found for example in [6], which also contains an extensive list of references.

measurements of the form and position of the Bragg peaks [1, 2]. Of the measurements on the technically important fcc structures, the work of Hinton, Schwartz, and Cohen [3] on silver and Hofer *et al* [4, 5] on copper gave values for stacking-fault densities, microstrains, and effective grain sizes for the above-mentioned structures electrolysed under certain conditions. On the other hand, electrolytic nickel has not been investigated in an equal manner. The measurements are in this case complicated by the above-mentioned tendency of nickel to develop relatively large, anisotropic strains during the electrolysis. The resulting changes in the positions of the Bragg peaks cause difficulty, especially in deformation-fault determinations according to the Paterson method [7], as shown by Otte *et al* [8] and Hinton, Schwartz, and Cohen [3] in other cases.

3. Object of the Present Work

In the present work, the structure of electrolytic nickel was investigated by X-ray diffraction using a special method for eliminating the effect of the anisotropic strains on the position of the Bragg peaks. The effect of the electrolysis pH upon the structure was studied by investigating samples produced from sulphate electrolytes with different pH values but otherwise identical.

4. Correction for the Anisotropic Strains

The method used by Otte *et al* [8] is developed further in the following to allow a correction of the effect of the anisotropic strains on the positions of the Bragg peaks.

The anisotropic strains cause a change in the position of every peak *hkl* by an amount which is proportional to the amount of strain in the direction perpendicular to the reflecting planes $\{hkl\}$. We get for the shift in the position of the Bragg peak $(h_1k_1l_1)$ identified by the value $p = h_1^2 + k_1^2 + l_1^2$ assuming that the strain perpendicular to $\{h_1k_1l_1\}$ plane is ϵ_p:

$$(\Delta 2\theta)'_p = -2\epsilon_p \tan\theta_p \qquad (\theta \text{ in radians}) \quad (1)$$

Some other peak $(h_2k_2l_2)$ with $q = h_2^2 + k_2^2 + l_2^2$ will be shifted by

$$(\Delta 2\theta)'_q = -2\epsilon_q \tan\theta_q$$

where $\epsilon_q \neq \epsilon_p$ because of the anisotropy. The net change in the angular separation of the two peaks is

$$(\Delta 2\theta)'_{p-q} = -2(\epsilon_p \tan\theta_p - \epsilon_q \tan\theta_q) \quad (2)$$

This change is superimposed upon the change in the angular distance of the peaks which is due to deformation faults. Following Warren's [1] notation, we can describe the latter change by $H_{p-q}.\alpha$, where α is the probability of deformation faults. Hence, the total change in the angular distance of the two peaks is finally $(\Delta 2\theta)_{p-q} = (\Delta 2\theta)'_{p-q} + H_{p-q}\alpha =$

$$-2(\epsilon_p \tan\theta_p - \epsilon_q \tan\theta_q) + H_{p-q}\alpha \qquad (3)$$

Since this expression contains three unknown quantities ϵ_p, ϵ_q and α, we need three observations, which must be chosen so that we do not introduce any additional strain components. In the case of a fcc structure, this can be accomplished by the following choice:

(i) measurement:		
$p = 4$	$(hkl) = 200$	$\epsilon_p = \epsilon_4$
$q = 3$	111	$\epsilon_q = \epsilon_3$
(ii) measurement:		
$p = 16$	400	$\epsilon_p = \epsilon_{16} = \epsilon_4$
$q = 12$	222	$\epsilon_q = \epsilon_{12} = \epsilon_3$
(iii) measurement:		
$p = 12$	222	$\epsilon_p = \epsilon_3 = \epsilon_q$
$q = 3$	111	

By inserting these values into the expression for $(\Delta 2\theta)_{p-q}$, we get three linear equations with respect to the unknowns ϵ_3, ϵ_4, and α. The solution of these equations is

$$\alpha = \frac{\begin{vmatrix} \tan\theta_4 & \tan\theta_3 & (\Delta 2\theta)_{4-3} \\ \tan\theta_{16} & \tan\theta_{12} & (\Delta 2\theta)_{6-12} \\ 0 & (\tan\theta_3 - \tan\theta_{12}) & (\Delta 2\theta)_{12-3} \end{vmatrix}}{\begin{vmatrix} \tan\theta_4 & \tan\theta_3 & H_{4-3} \\ \tan\theta_{16} & \tan\theta_{12} & H_{16-42} \\ 0 & (\tan\theta_3 - \tan\theta_{12}) & H_{12-3} \end{vmatrix}} \qquad (4)$$

and similar expressions for ϵ_3 and ϵ_4.

5. Samples

Samples were prepared by electroplating nickel onto a thick copper plate. The conditions of electrolysis are given in table I. The thickness of the electroplated layer was in each case about 0.2 mm, which is sufficient to allow the defect structure to develop completely.

The diffraction measurements described below were first made for each sample at room temperature. The samples were then heat treated according to the programme given in table II, the diffraction measurements being repeated after each heat treatment. A series of measurements was thus obtained, each measurement corres-

TABLE I Conditions of the electrolysis.

Base plate: Copper	
Temperature: 23° C	
Current density: 10 mA/cm² (dc)	
Analysis of the electrolyte:	
Ni^{++}	85 g/l
Cu^{++}	0.03 mg/l
Pb^{++}	0.25 mg/l
Zn^{++}	0.20 mg/l
Fe^{++}	0.38 mg/l
H_3BO_3	19 g/l
Na_2SO_4	125 g/l

TABLE II Treatment of the samples (m = measurement).

Storage at room temperature (several months) → m → 100° C, 1 h → m → 200° C, 1 h → m → 300° C, 1 h → m → 350° C, 1 h → m → 400° C, 1 h → m → 450° C, 1 h → m → 500° C, 1 h → m → 550° C, 1 h → m → 600° C, 1 h → m

ponding to a certain combination of pH and heat treatment.

6. Measurements

The measurements were made with a Philips wide-angle goniometer using CuKα radiation, scintillation counter, and a rate meter connected to a recorder. The goniometer speed was $\frac{1}{4}$ or $\frac{1}{8}$ deg/min. The measuring geometry used was: divergence and antiscatter slits, 1 deg; receiving slit, 0.1 or 0.2 mm. The chart speed was 400 mm/h. The following peaks were recorded: (111), (200), (222), (400).

7. Calculations

After subtracting the background, a Stokes correction [1] was first applied to the observed peak profiles by measuring the corresponding profiles from a well-annealed, coarse-grain nickel specimen. The conditions stipulated by Guinier ([9], p. 146) for the applicability of Stokes' correction were hereby fulfilled, except for the profiles given by the least faulted samples, for which the correction probably was not very accurate. In connexion with the correction, a Fourier analysis of the peak profiles was performed according to the well-known methods described in [1].

From the positions of the peak maxima, the *deformation*-fault density, α, and the long-range strains, ϵ, in the two principal directions <100> (=ϵ_4) and <111> (=ϵ_3) were calculated from (4) and the similar expressions for ϵ_4 and ϵ_3. A sufficiently accurate determination of the maximum position of the peaks (222) and (400) proved difficult because of the smallness of the peaks and their large 2θ-values. Centres of gravity were therefore used instead of the maxima for these peaks. This change was justified by the high degree of symmetry of the peaks because of the relative smallness of the twin-fault densities observed (see below; cf. [2]).

The density of *twin* faults, β, was determined from the difference between the peak maximum and the centre of gravity according to Cohen and Wagner [2]. The pair (111)–(200) was used in the determination.

The average, coherent, domain size D_{eff} was determined from an extrapolation of the tangent of the A_L versus L curve to the L axis, according to the Fourier analysis method described in [1]. This was done for the two principal directions <100> and <111>. The relative accuracy of this method is of the order of 20% if D_{eff} is a few hundred Ångströms, but becomes very poor at about 1000 to 2000 Å. At such large domain sizes, the broadening of the observed profile due to this cause is too small to be accurately separated from the superimposed instrumental broadening.

8. Results

It was found that the solution (4) of the three equations (3) into which the observed values of $(\Delta 2\theta)_{p-q}$ were inserted gave values of deformation-fault densities, α, scattering around zero by an amount which was within the estimated accuracy of the method $\Delta\alpha \approx 2 \times 10^{-3}$. It was also found in most cases that only about 10 to 20% of the peak shift $(\Delta 2\theta)_{p-q}$ in (3) was due to the last term $H_{p-q}\alpha$. Hence, the main reason for the observed peak shifts were the macrostresses. It can be concluded that very few deformation faults were produced by the electrolysis or the subsequent heat treatment regardless of the pH. This result is in agreement with the observations by Hofer and Hintermann [5] for electrolysed copper and by Hinton, Schwartz and Cohen [3] for silver. Somewhat higher values ($\alpha \approx 5 \cdot 10^{-3}$) were found by Wagner [10] for cold-worked nickel at room temperature, whereas Michell and Haig [12] found no deformation faults.

The results for the twin-fault densities, β, are given in figs. 1 and 2. It is seen that fault density values exceeding the measuring accuracy ($\Delta\beta \approx 2 \times 10^{-3}$) are found, although the measured

effects are only slightly above the limit of detectability. Considering the averages, it is clear, however, that a maximum of the twin-fault density is found in the medium pH range 3 to 4 for samples kept at room temperature. The faults disappear easily in a heat treatment, so that 100° C is enough to remove the excess found in the medium pH range. At 300° C, the fault density is already stabilised to a very low value.

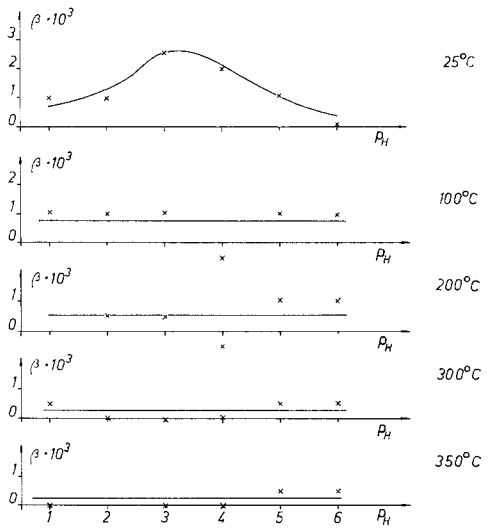

Figure 1 Density of twin faults as a function of the pH of the bath for samples heat treated at successively increasing temperatures.

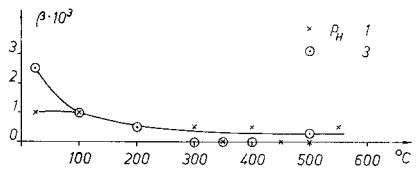

Figure 2 Density of twin faults in two samples as functions of the heat-treatment temperature.

The values of β found are to be compared on the one hand with the much higher values (up to 2×10^{-2}) found by Hofer and Hintermann [5] for electrolytic copper using a thiourea additive to the electrolyte. On the other hand, no measureable amounts of twin faults were found by Wagner for cold-worked nickel [10]. The latter result demonstrates the relatively high energy associated with a twin fault in nickel, which explains why in electrolysed samples also these faults are less frequent than in the former cases.

The calculated macrostrains ϵ_{100} are given as functions of annealing temperature and pH in figs. 3 and 4. Compressive strains clearly above the limit of detectability ($\approx 5 \times 10^{-4}$) are found in the $<100>$ direction in the pH region 3 to 6 at room temperature. The strains disappear in the temperature region 100 to 300° C, the stability of the strains increasing with the bath pH. Below pH $\approx$ 3, no measurable strains were found.

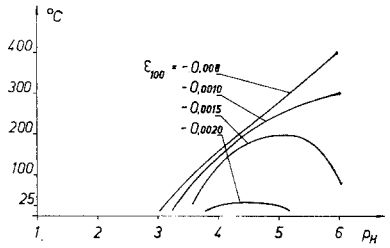

Figure 3 Contour curves of the strain in the direction along the cube edge ϵ_{100} as a function of the bath pH and the heat-treatment temperature.

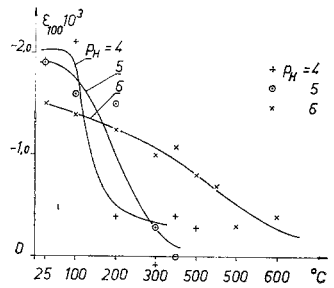

Figure 4 Strain ϵ_{100} as a function of the heat-treatment temperature for the samples deposited at pH = 4, 5, 6.

On the other hand, measurements of ϵ_{111} did not give any systematic values above the limit of detectability in any sample. Hence, it can be concluded that no macrostrains along the cube diagonal could be detected.

The average domain sizes D_{eff} are given as functions of pH and the annealing temperature in figs. 5 and 6. It is seen that the behaviour of the domain size depends strongly on the bath pH. At relatively high pH ($\approx$4 to 5), the average domain size is not significantly different in the two principal directions, if we take into account the limitations of the accuracy of the measurement. This applies to all heat treatments. At low pH ($\lesssim$3), we find that the domain size is considerably smaller in $<100>$ direction than in $<111>$ direction, the difference being maintained with increasing heat treatment. The different behaviour of D_{eff} for different pH is illustrated clearly in fig. 7, which shows the domain sizes as functions of temperature for

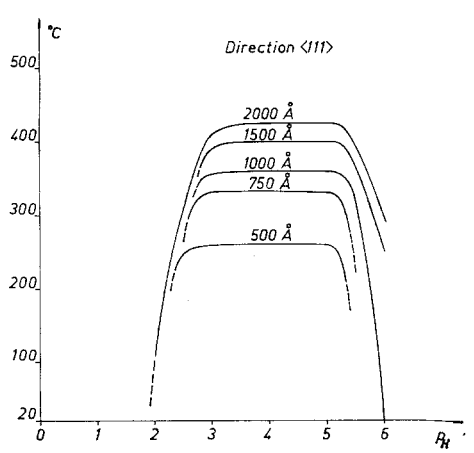

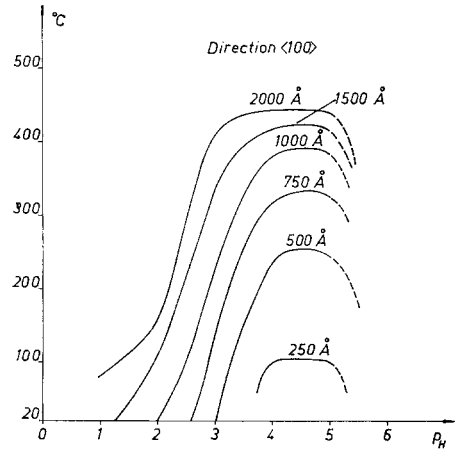

Figures 5 and 6 Contour curves of the average domain sizes D_{eff} in directions <111> and <100> as functions of the bath pH and the heat-treatment temperature.

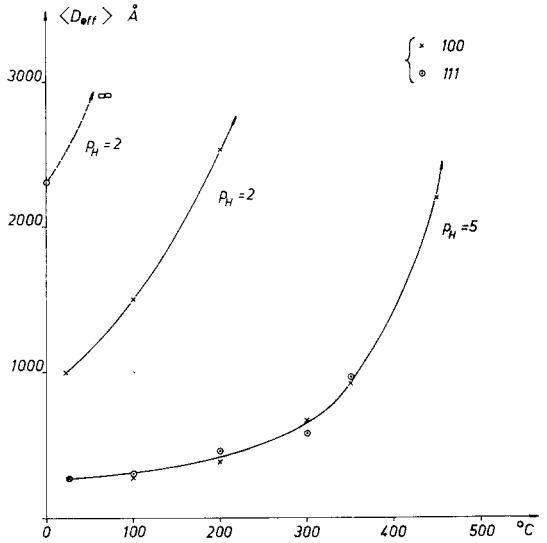

Figure 7 The average domain sizes D_{eff} along the cube edge (X) and the diagonal (⊙) as a function of the heat-treatment temperature for samples deposited at pH = 2 and 5.

pH = 2 and pH = 5. We also see that the onset of a rapid increase in D_{eff} takes place at $t \gtrsim 300°$ C for pH = 5, whereas the corresponding temperature is much lower for pH = 2, and the growth is more gradual. The ratio $(D_{eff})_{111}/(D_{eff})_{100}$ is ≈ 1 for pH = 5. For pH = 2, the ratio is clearly larger at room temperature, although the estimate is very rough because of the poor accuracy of the method for such large values of D_{eff} (see above).

The results on the domain growth agree qualitatively with the results of Hofer and Hintermann [5] for copper electrodeposited in the presence of thiourea. The negative strains found in the <100> direction can be compared with observations by Nishihara and Tsuda [13]. They found the overall strains to be compressive and to increase with pH.

9. Discussion

The results obtained for the twin faults can be explained according to the following model. The boundary regions of the twin faults always created by the electrolysis are locked by some kind of point defects in the lattice which prevent the annihilation of the faults. This would otherwise take place because of the high, twin-fault energy in nickel. If the temperature is raised to about 100° C, the mobility of the defects becomes sufficiently large to permit their departure, after which the faults are annihilated. A plausible explanation is that the locking action is created by nickel atoms pushed into interstitial positions.

The activation energy for the diffusion of interstitials in nickel is not known, but in copper it is estimated to be of the order of 0.1 eV ([11], p. 33) which is compatible with the observed temperature region (near 100° C) for the removal of twin faults. Rough estimates of the binding energy between interstitials and edge dislocations give results of the same order of magnitude ([11], p. 72).

The behaviour of the macroscopic strains ϵ_{100} and of the factors reducing the average domain size D_{eff} are very similar with pH: both are the more pronounced, the higher the pH, up to pH $\approx$ 6. Both effects also persist to roughly the same temperature, which is

considerably higher than the disappearing temperature of the twin faults. All this points to the same cause for both phenomena, viz. co-deposition of colloidal hydroxide, which can be expected to occur in the pH region 3 to 6 but not below pH $\approx$ 3, since colloidal hydroxide becomes unstable ([6], p. 636)*. Once deposited in the nickel lattice, the hydroxide groups can be expected to diffuse much more slowly than interstitials, which would explain the persistence of both above-mentioned phenomena up to temperatures higher than those needed for the disappearance of the twin faults.

As to the detailed mechanism of the deposition of the colloidal hydroxide, nothing definite can be said on the basis of the results reported above. The different behaviour of the strains along the cube edge and the diagonal is, however, interesting. On the other hand, the average domain size is nevertheless essentially the same in <100> and <111> directions for the samples with presumably abundant deposition of the colloidal hydroxide.

10. Conclusion

The results obtained confirm the view of Macnaughtan *et al* [14], according to which the colloidal hydroxide, rather than hydrogen, is the controlling factor of the quality of the deposit. Possibly, hydrogen is responsible for the creation of the interstitials which it is suggested cause the twin faults found, but the twin faults are obviously not very important from the point of view of the technologically important properties, above all the hardness and the macroscopic stresses. The strains associated with these stresses are seen to behave in a manner different from the twin faults, and are most probably caused by colloidal hydroxide.

Acknowledgements

Financial aid from the Research Council for Engineering and Science of the State of Finland is gratefully acknowledged. The author is also grateful to Messrs I. Ala-Vainio and H. Torvela for their assistance in measurements and numerical calculations. A part of the experiments was done by Mr Ala-Vainio for an undergraduate (engineer diploma) thesis.

Thanks are also due to the Harjavalta Nickel Plant of the Outokumpu Co for preparing the samples.

References

1. B. E. WARREN, *Progress in Metal Physics* **8** (1959) 196.
2. J. B. COHEN and C. N. J. WAGNER, *J. Appl. Phys.* **33** (1962) 2073.
3. R. W. HINTON, L. H. SCHWARTZ, and J. B. COHEN, *J. Electrochem. Soc.* **110** (1963) 103.
4. E. M. HOFER and P. JAVET, *Helvetica Physica Acta* **35** (1962) 369.
5. E. M. HOFER and H. E. HINTERMANN, *J. Electrochem. Soc.* **112** (1965) 167.
6. H. FISCHER, "Elektrolytische Abscheidung und Elektrokristallisation von Metallen" (Springer, Berlin, 1954).
7. M. S. PATERSON, *J. Appl. Phys.* **23** (1952) 805.
8. H. M. OTTE, D. O. WELCH, and G. F. BOLLING, *Phil. Mag.* **8** (1963) 345.
9. A. GUINIER, "X-ray Diffraction" (Freeman & Co, San Francisco, 1963).
10. C. N. J. WAGNER, *Revue de Metallurgie* **55** (1958) 1171.
11. A. C. DAMASK and G. J. DIENES, "Point Defects in Metals" (Gordon and Breach, New York, 1963).
12. D. MICHELL and F. D. HAIG, *Phil. Mag.* **2** (1957) 15.
13. K. NISHIHARA and S. TSUDA, *Trans. Min. Met. Alumni Assoc.* **14** (1962) 397.
14. D. S. MACNAUGHTAN, G. E. GORDON, and R. A. F. HAMMOND, *Trans. Faraday Soc.* **29** (1933) 729.

*In fact, colloidal hydroxides should disappear if pH $\lesssim$ 4. The pH can, however, be expected to be considerably higher in the neighbourhood of the cathode than in the electrolyte. This explains why the effect of the colloidal hydroxide can be expected even at pH values somewhat lower.